A method to estimate the photovoltaic penetration and capital costs of greenfield projects

Author(s):
Shi, Zhongming; Fonseca, Jimeno A.; Schlueter, Arno

Publication date:
2020

Permanent link:
https://doi.org/10.3929/ethz-b-000391820

Estimating solar energy penetration and the costs at the district scale with block typologies in high-density cities

Zhongming Shi [a, b, *], Jimeno A. Fonseca [a,b], Arno Schlueter [a,b]

[a] Future Cities Laboratory, Singapore-ETH Centre, 1 Create Way, CREATE Tower, Singapore 138602, Singapore
[b] Architecture and Building Systems, ETH Zurich, Stefano-Franscini-Platz 1, Zurich 8093, Switzerland

Abstract
Renewable energy potential is becoming one of the critical criteria for evaluating an urban or architectural project. Rather than at the downstream of a project's a series of the development phases, energy considerations shall be included at the early stage of the urban design processes. Assessment on the renewable energy potential, solar energy, for example, requires to know the envelopes of building volumes for PV installations. However, usually, no design decisions are made at the early design stages of the greenfield project. This work proposed a method of estimating the renewable energy potential with design generated based on vernacular block typologies in Grasshopper/Rhinoceros. Besides, this paper introduced a method to produce such block typologies. Energy simulations were made with the City Energy Analyst tool. We made a demonstration in the context of Singapore. As a by-product, we derived an inventory of 18 block typologies through six case studies on the high-density areas of Singapore. Urban designers can use this method for renewable energy potential estimation to test the feasibility of their energy performance targets. Vice versa, this paper also provides a means to interpret the results into design suggestions aiming at a high or targeted renewable energy potential.

Keywords: renewable energy potential; urban form; block typology; energy-driven urban design; Singapore

1. Introduction

Cities are responsible for approximately 75% of the primary energy consumptions and 60% of the greenhouse emissions of the world (UN-Habitat, 2012). Massive urbanization continues to happen (Seto et al., 2012), as the urban population keeps increasing and there is no sign of slowing (United Nations, 2018). Buildings are one of the highest energy-consuming sectors of cities. As a result, people have been constantly investing on increasing the building energy efficiency (Climate Leadership Group, 2019). The use of renewable energy improves the energy efficiency. A common goal shared among countries is to integrate significant shares of renewable energy into their energy mix (Eco-Business, n.d.; Shields & Miller, 2017). However, the challenge lies on how to set an achievable target of renewable energy integration at the very early stage of an urban development, when energy-driven design strategies are the most effective in increasing the energy efficiency (IEA ECBCS Annex51 - Subtask B, 2012; Mohajeri et al., 2016).

Moreover, the challenge also lies on how to set the urban design constraints on the relvant urban attributes to achieve the given goal of renewable energy integration. For example, some of the potenital of renewable energy in cities, like the photovoltaic electricity generation, is highly dependent on the building geometries and the surrounding urban contexts (Lau et al., 2017). Both of these affect the availability of building façades for solar photovoltaic installations and the mutual shading of the building geometries. However, at the very early stage of an urban development project, there is usually a lack of such design inputs for the renewable energy potential estimation. Many have studied the interdependencies between the given urban form and its renewable energy potential (Vartholomaios, 2015; Vulkan et al., 2018; Zhang et al., 2019). Nevertheless, in this work, we intend to address this knowledge gap that few studies have touched the estimation of renewable energy potential at an urban development stage in absence of design inputs.

Block typologies are widely used for urban morphological studies on urban airflows (Merlier et al., 2018), daylighting (Saratsis et al., 2017), and urban vitality (Ye et al., 2018). Concerning studies on energy efficiency and renewable energy potential, block typologies are of great popularity as well. Natanian et al. demonstrated a parametric workflow to optimizing energy balance, environmental quality, and urban form with five types of generic building/block typologies in the context of Tel Aviv (Natanian et al., 2019). To create an urban context in the simulations, each block typology is duplicated to produce a grid of nine identical blocks with the targeted block in the center. Other urban inputs, like the street width, window to wall ratio, conform to the local design regulations and codes. The finding reveals that certain block typology and density favor the balance between solar energy potential, cooling energy demand, and daylight availability. Zhang et al. conducted a series of simulations on six block typologies in Singapore and gave out urban design strategies for higher renewable energy potential (Zhang et al., 2019). The block typologies used were derived from generic building patterns. The source and the relevance of such building patterns to the contexts of Singapore was not explained. The result reveals that certain block typologies can significantly improve the building energy use efficiency and solar energy harvesting. Similarly, generic block typologies are used in urban morphological studies for low carbon emissions (Li et al., 2016) and heating/cooling energy consumptions (Vartholomaios, 2017) in various locations and climates.

In contrast, a series of studies used the actual built urban form for the studies on urban solar energy potential. A common method shared by such studies is selecting certain sizes of exisiting districts in multiple neighbourhoods of a city for solar energy simulations (Chatzipoulka et al., 2016; Mohajeri et al., 2016). Since the harvesting of certain types of renewable energy, like solar energy, is subject to the urban form, such a method using the actual built urban form can lead to more accurate simulation results than that using the generic block typologies. Comparing to that using the identical block typologies as the surrounding urban contexts, using the actual built urban form provides a much more diverse surrounding and increase the simulation accuracy. In addition, the actual built urban form reflects and respects the vernacular way of building design and people's living, which increases the results' potential for being integrated in the local urban or building design processes. However, the main drawback lies in the high computational expenses for the excessive and unnecessary details for the design generation and renewable energy potential estimation at the early stage of the design processes.

As a compromise, some studies adopt a method that meets in the middle between using the actual built urban and generic urban form. For example, Vulkan et al. used a series of blocks (clusters of building typologies) to demonstrate an algorithm for spatiotemporal calculation of shadows on building surfaces (Vulkan et al., 2018). These context-specific typologies were retrieved from two actual built neighborhoods in Israel. Tsirigoti and Tsikaloudki studied the relationships between urban form and energy efficiency with 28 block typologies in Greek Cities (Tsirigoti & Tsikaloudaki, 2018). Each block consists of a number of typical buildings retrieved from a database of typical building typologies. In terms of experimental design, the latter

adopts the method of duplicating the indentical block typology surrounding the targeted block typology in the center, while the former adopts a method of using different blocks shadowing each other to create a complex and irregular urban contexts. In terms of scale, both of these two studies focus on single block typologies at the building-block level, while the interrelationships between blocks at the block-district scale were not studied.

In the studies on renewable energy potential and energy efficiency with block typologies mentioned above, researchers selected various parameters of design inputs for describing the configuration of an individual block typology (Li et al., 2016; Natanian et al., 2019; Vartholomaios, 2017; Zhang et al., 2019). They share four common parameters of basic design inputs – block dimension, land use, building footprint, and density. The block dimension means the length and width of the identical blocks. The land use included residential, offices, commercial, etc., which are fundamental for energy demand forecasting. The building footprint derived from the generic building patterns, like the courtyard, slab, etc. (Martin & March, 1972; Ratti et al., 2003; Steemers et al., 1997). The density came in two forms across the four studies, including floor area ratio and number of floors. Except for the building footprint, the other three parameters are often commonly used in a city's master plan for controls at the early stage of urban development processes (Urban Redevelopment Authority, 2014b). Site coverage ratio is often witnessed to be used as a control over the building footprint design in a city's urban design regulations. The presences of block width and length, land use, building pattern, floor area ratio, and site coverage ratio suffice to describe the configuration of an individual block typology.

Regarding the aspects of performance assessment on renewable energy potential, PV generation, solar thermal yield, solar radiation, and wind flow were listed by Natanian et al. in a review of 50 recent studies on evaluating urban design parameters for environmental impacts (Natanian et al., 2019). At the district scale, a a metric called the load match (LM) index emerged as an effective way as an perforamance assessment indicator for the use of renewable energy (Sartori et al., 2012; Voss et al., 2010; Widén et al., 2009). It reflects the temporal (hourly, daily, and yealy) energy demand fulfilled by the renewable energy production on-site. However, few study has taken the expenditure on renewable energy conversion technologies into considerations, while cost-to-value is of great importance in implementing the harvesting of renewable energy.

This study aims at introducing a method to estimate the renewable energy potential of a district at its early stage of urban design processes with block typologies. Based on the literature studies above, the block typologies and performance assessment metrics have to fuill the following requirements. Regarding the block typologies, they shall reflect the vernacular contexts, and the surrounding buildings in the simulations shall be diverse. Regarding the metrics of performance assessment, besides that merely measures renewable energy potential, the expenditures on the capital invesmention and operation on the technologies shall be considered. The application of this method shall be demonstrated to answer questions like: What is the highest achieveable renewable energy potential as well as the corresponding expenditures of a district lacking design inputs at its early stage of urban design processes?

In section 2 we introduce the methodology of this paper. In section 3, we apply the method through a demonstration in the context of Singapore. Later on, in section 4, we extend a discussion of the study. Finally, in Section 5, we present our conclusions and final remarks.

Nomenclature

$CAPEX$	capital expenditure [USD]
$aCAPEX$	annualized capital expenditure [USD]
$aOPEX$	annual operational expenditure [USD]
CEA	City Energy Analyst
UBG	Urban Block Generator
PV	photovoltaic
STC	standard test conditions
I	irradiance
η	efficiency
i	interest rate

2. Methods

The four-step workflow for our method of estimating the renewable energy potential and the expenditures for a greenfield project is depicted in Figure 1. In addition, the figure illustrates the relationships between the four steps. Section 2.1 collected the data for making the inventory of block typologies in the Second Step (Section 2.2). The tool used for processing the data were ArcGIS (Citation) and JMP Pro 13 (SAS Institute Inc., 2016). The Third Step (Section 2.3) parametrized the block typologies on the platform of Grasshopper (Robert McNeel & Associates, n.d.). The Fourth Step (Section 2.4) introduced the methods of assessing the renewable energy potential and corresponding expenditures with the City Energy Analyst (CEA) (The CEA team, 2018).

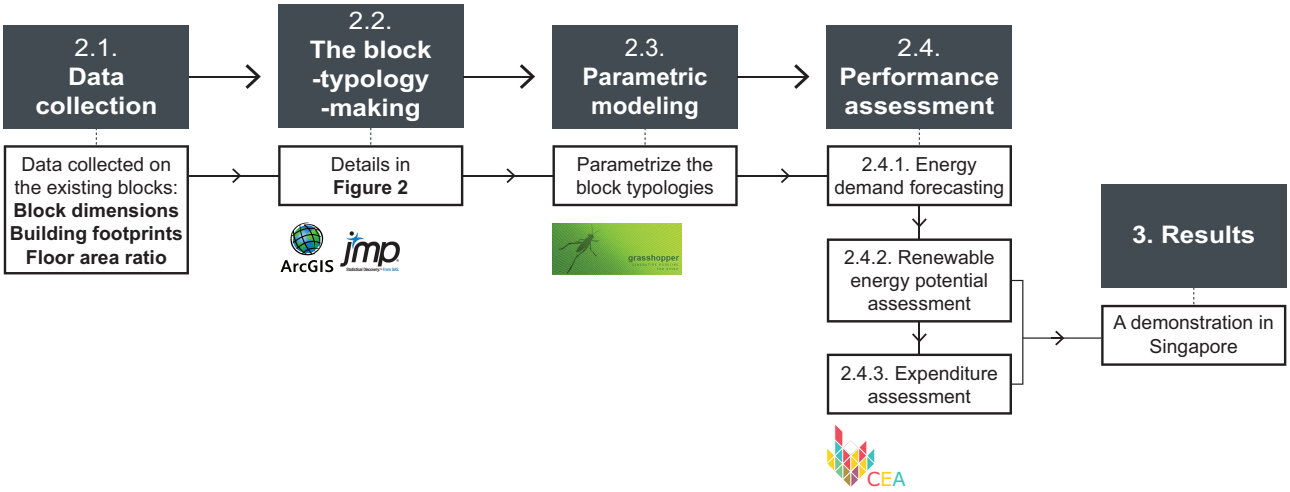

Figure 1. The four-step workflow and the tools used in Section 2, as well as their relationships with the demonstration in Singapore through Section 3.

2.1. Data collection

Before all, there are three streams of basic data required. First is the data needed to produce the vernacular block typologies, which include the geometries of the street layout, blocks, building footprints and the information on building intensity. Usually, such data can be acquired from the master plan from the local planning authority or OpenStreetMap. Second is the geometries of the immediate urban context, if any, that surrounds the site of the greenfield project. Last is the data for the renewable energy potential assessment, which include, for example, the occupancies for energy demand forecasting and the specs of the energy supply technologies. Such data in this research are retrieved through literature studies or the database of the simulation programs. The data sources for the demonsration in Singapore are detailed in Section 3.

2.2. The block-typology-making

To make the block typologies, a series of classification and filtering (see Figure 2) is conducted based on a hierarchy following the order of block dimensions at the block level (2.2.1) as well as building patterns, and floor area ratio, and site coverage ratio at the building level (2.2.2). The dimensions of blocks are shaped by the street layout, which, together with floor area ratio, is usually the most basic urban design attributes defined in a master plan. Building patterns and site coverage are another two basic design attributes that define the buildings in a block.

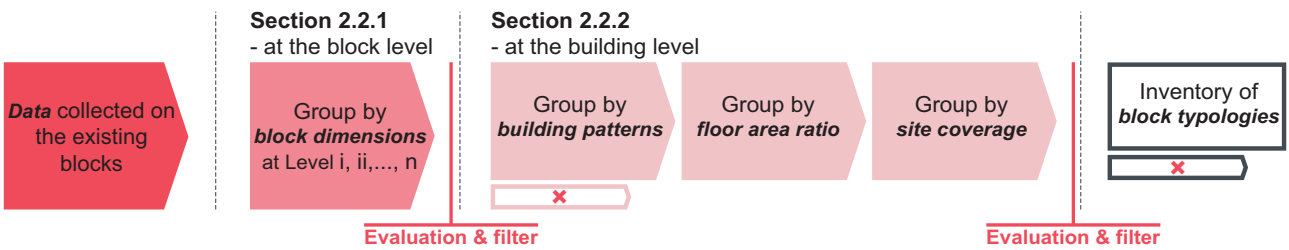

Figure 2. The method proposed in this study for the block-typology making.

2.2.1. At the block level

Group by block dimensions

The blocks retrieved from the master plan are usually of great difference and irregularity. To classify them with similar attributes, we adopt the clustering method of *k*-means, which has been used in several studies on urban form classifications (Montenegro et al., 2009; Schirmer & Axhausen, 2015; Vialard, 2013). We execute k-means clustering with JMP Pro 13 (SAS Institute Inc., 2016). The two factors used in the clustering are block area and elongation (Shi et al., 2019; Vialard, 2013). The former measures the size of the block while the latter measures the shape of the block. Details about how to calculate the block elongation can be found in Appendix A. However, the decision of the number of clusters requires several trail clustering. Too many clusters create too many small groups with similar attributes while too few clusters cannot provide enough differentiation. Should the streets come in hierarchy with multiple levels, the block dimensions can be grouped in multiple levels that correspond to the level of streets. For example, arterial streets define super blocks and minor streets define smaller blocks.

Evaluation and filtering

The blocks retrieved from the master plan may contain ones of great irregularity in either the size or the shape. It is usually because of the special terrains or preserved buildings that make the blocks either too big or too long, for example. However, such irregular blocks should not be replicated in the design generation. The groups of blocks produced above are subject to evaluation and filtering. The method of evaluating and filtering used in this research is as follows. In high-density cities, the connectivity of the street network is of great importance, which can be measured by the intersection density (Ellis et al., 2016). See **Equation 1** for its calculation. An intersection means where more than two links of the street network join. In a grid street pattern with a reasonable street width, to increase the intersection density for higher connectivity means to allocate more land to be occupied by the streets, which we use street area ratio to measure (See **Equation 2**). Since land scarcity is among the top challenges in high-density cities, an obvious trade-off between the intersection density and the street area ratio can be foreseen.

$$Intersection\ density = \frac{number\ of\ intersections}{site\ area} \quad (1)$$

$$Street\ area\ ratio = \frac{street\ area}{site\ area} \quad (2)$$

To decide what a good compromise between the intersection density and street area ratio should be, we refer to a variety of different block dimensions of cities with grid street plans. We retrieve the block dimensions using Google Earth and apply them together with the clusters of blocks produced above to the same site of study. Then we calculate their intersection density and street area ratio. Figure 3 gives out an example of the results with the typical North American Cities in circle and the clusters of block dimension acquired above in cross. Out of the nine cluster only three red crosses fall into the shaded area, and the rest is located relatively far away for either comparatively low intersection density or high street area ratio. For this example in Figure 3, three groups are kept and will be considered in further classifications, and the other six are excluded as either their size or shape causes poor connectivity or utilizes excessive land for streets.

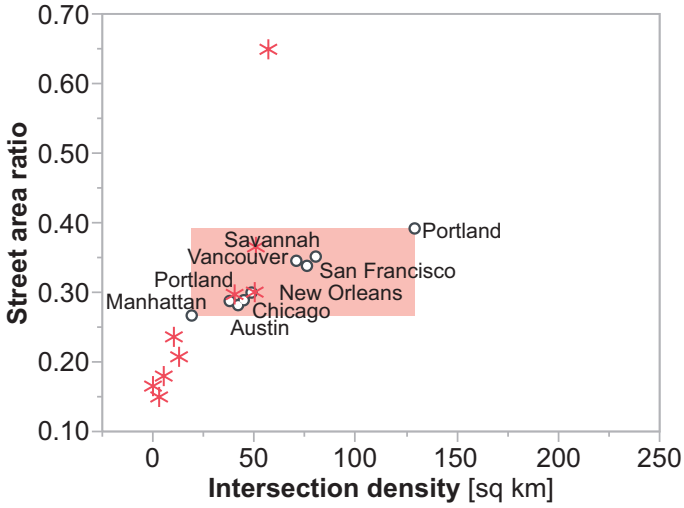

Figure 3. Example evaluation of the groups of blocks by street area ratio and intersection density.

2.2.2. At the building level

Group by building patterns
In this study, we view all the individual building patterns within each block combined as a whole building pattern of each block. Based on the six generic urban forms by Martin and March (Martin & March, 1972; Ratti et al., 2003; Steemers et al., 1997), we extracted seven basic building patterns for blocks in Figure 4. We categorize the blocks of the remaining groups from the previous step of clustering by these seven basic building pattern types. Given a reasonable quantity of blocks, this work can be processed manually by an urban designer. Should the data of building footprints retrieved from the master plan or the OpenStreetMap be incomplete, more can be acquired from the images on Google Earth.

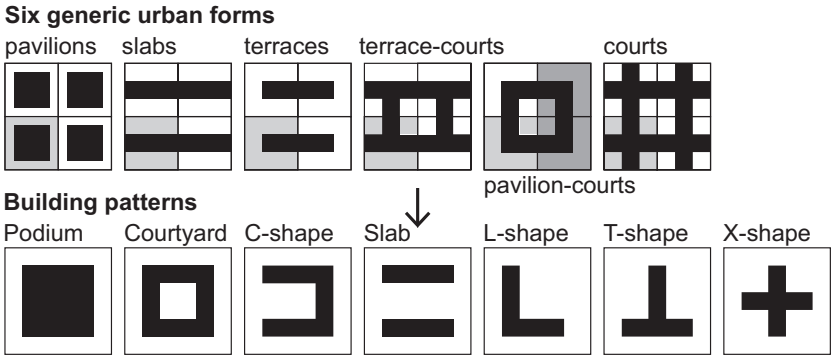

Figure 4. Seven basic building patterns extracted from the six generic urban forms.

Group by floor area ratio and site coverage ratio
After the classifications of block dimensions and building patterns, now we conduct further classifications based on the floor area ratio (**Equation 3**) and the site coverage (**Equation 4**). Floor area ratio and site coverage are two common building metrics that measure the vertical and horizontal building density. We group the blocks within each group if they have a close floor area ratio and site coverage.

$$Floor\ area\ ratio = \frac{gross\ floor\ area}{site\ area} \quad (3)$$

$$Site\ coverage = \frac{building\ footprint\ area}{site\ area} \quad (4)$$

Evaluation and filtering
In this round of evaluation and filtering, we remove the groups of blocks that meet one or more of the following three criteria. The group of blocks should be excluded from the final inventory of block typologies, if the block is vacant or partially vacant or the data of the building patterns are missing. The group of blocks should be excluded, if the average floor area ratio of the blocks inside the group is under the threshold as high-density. The group should be excluded, if it only contains one block inside. After this process of filtering, the remaining groups of blocks make up the final inventory of block typologies.

2.3. Parametric modeling in Grasshopper
What is Grasshopper?
Why we need to parametrize?

2.4. Performance assessment
In this research, we use the CEA 2.9.0 (The CEA team, 2018) to simulate total energy demand and electricity generation by the PV panels. Besides the design inputs (building geometries and land use ratios), all other inputs are from the CEA database. It contains the local building envelope parameters, weather conditions, and the occupancy schedules of Singapore. Besides the total energy demand and the PV electricity productions, results of the CEA simulations include the number of people on site, the area and the costs of PV panel installations. The City Energy Analyst (CEA) (Fonseca et al., 2016), an open-source energy simulation toolbox, simulates building energy demand and energy supply technology operation. Assuming a steady-state operation, CEA performs simulations with hourly steps over a year. Objectives

2.4.1. Energy demand forecasting

2.4.2. Renewable energy potential estimation

The renewable energy share (RES), ranging from 0 to 1, of a block is defined as the ratio of the total energy consumption happened within the block fulfilled by the renewable energy produced in that block. RES is calculated in **Equation 5**. The total energy consumption consists of three parts: the space cooling demand ($\mathrm{Q_{sc}}$ [KWh]), the electricity demand ($\mathrm{El_e}$ [KWh]), and domestic hot water (DHW) demand ($\mathrm{Q_{dhw}}$[KWh]). Accordingly, the total energy consumption met by the energy supplies from different renewable energy resources also consists of three corresponding parts.

$$\mathrm{RES} = \frac{\sum_{k=1}^{n}(\mathrm{Q_{sc,k}+El_{e,k}+Q_{dhw,k}})}{\mathrm{Q_{sc}+El_e+Q_{dhw}}} \quad (5)$$

2.4.3. Expenditures on photovoltaic panels

Besides achieving high renewable energy potential, the costs of the conversion technologies for renewable energy is also of great importance. This research uses the annualized capital cost (aCAPEX) and operational cost (OPEX) per gross floor area (GFA) to measure the costs.

For PV panels in this research, generic monocrystalline panels are used. The calculations of aCAPEX [USD] and OPEX [USD] of the PV are performed by CEA, based on **Equation 6** through **9** and Table 1 from the CEA database (The CEA team, 2018). **Equation 6** calculates the nominal installed capacity ($\mathrm{P_n}$ [W]) with the area of the PV installed ($\mathrm{S_{pv}}$ [sqm]), the solar irradiance at the standard test conditions (STC) ($\mathrm{I_{STC}}$ [W/sqm]), and the nominal efficiency of the PV ($\mathrm{\eta_n}$). $\mathrm{I_{STC}}$ equals 1'000 and $\mathrm{\eta_n}$ equals 0.16. In **Equation 8**, aCAPEX is calculated with CAPEX, annual interest rate (i), and the lifetime of the PV (LT). IR is set at 5% and LT is assumed as 20 years.

$$P_n = S_{pv} \cdot I_{STC} \cdot \eta_n \quad (6)$$

$$CAPEX_{technology} = a + b \cdot {P_n}^c + (d + e \cdot P_n) \cdot log\,(P_n) \quad (7)$$

$$aCAPEX_{technology} = CAPEX_{technology} \cdot \frac{i(1+i)^n}{(1+i)^n - 1} \quad (8)$$

$$OPEX_{technology} = \frac{aCAPEX_{technology}}{100} \quad (9)$$

Table 1. Parameters in the calculations of the costs on photovoltaic panels.

Nominal installed capacity (P_n [W])	*a*	*b*	*c*	*d*	*e*
$1 \le P_n < 10'000$	0	3.6	1	0	0
$10'000 \le P_n < 200'000$	0	2.6	1	0	0
$200'000 \le P_n$	0	2.6	1	0	0

3. Results: a demonstration in Singapore

3.1. Data collection

The pool of blocks sampled for the block-typology-making comes from the six high-density areas in Singapore: Downtown (DT), Jurong East (JE), One North (ON), Paya Lebar (PL), Tampines (TP), and Woodlands (WL). These six areas are selected for their high-density planned or envisioned by the planning authority of Singapore (Urban Redevelopment Authority, 2014a, 2014b). We use the subplanning areas of the Singapore Master Plan to limit the boundaries of these six areas (Urban Redevelopment Authority, 2014b). Figure 5 shows the containing blocks and the locations of the six selected SG HDMU areas. The street layouts, blocks, and the FARs come from the Singapore Master Plan 2014 (Urban Redevelopment Authority, 2014b, 2014c) and the shapefiles of the building footprints are downloaded from the OpenStreetMap (OpenStreetMap, 2017).

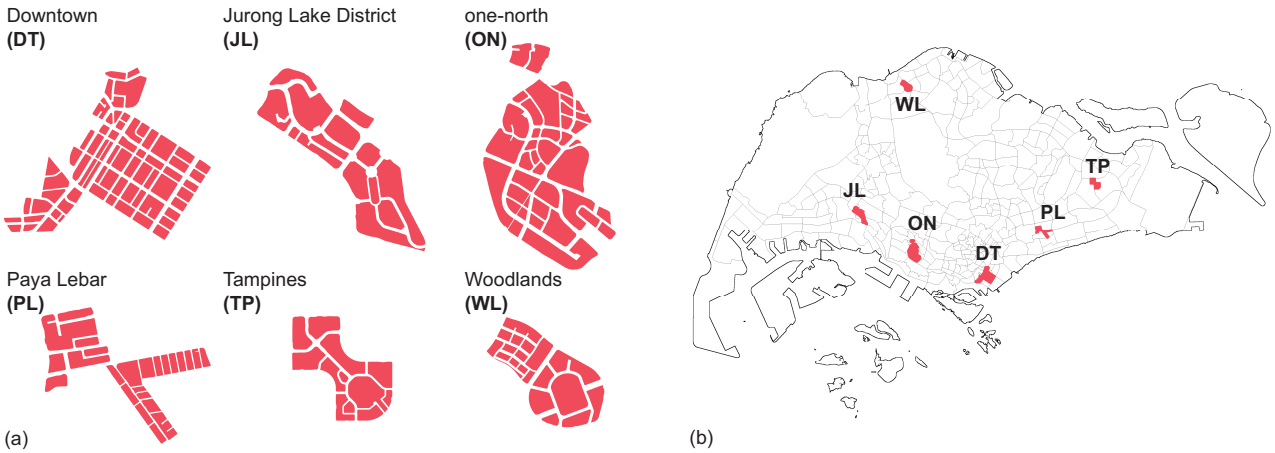

Figure 5. Six HDMU areas: blocks (a) and location (b).

3.2. The block typologies in high-density areas of Singapore

The pool of blocks from the six high-density areas of Singapore contains 178 different and irregular blocks. Based on the method proposed in Chapter 2.2, an inventory of 18 block typologies is made. The details of the process are as follows.

3.2.1.The district street layout prototype

As stated above, we inherit the district street layout prototype from a recent study through the same six study areas in Singapore (Shi et al., 2019). The result is illustrated in Figure 6. There are two levels of streets: arterial and minor streets. Arterial streets have a minimum width of 31.6 m, and minor streets have a minimum width of 15.8 m. Arterial streets first divide the site into bigger blocks, which are around 588 m long and 320 m wide. Then, minor streets further divide the bigger blocks into blocks. In this paper, we assume all the blocks are homogeneous.

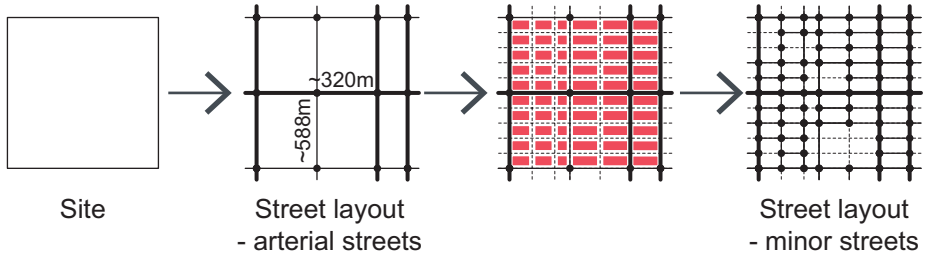

Figure 6. The district street layout prototype in the high-density areas of Singapore; modified based on (Shi et al., 2019).

3.2.2. Groups by block dimensions

Figure 7 illustrates the nine clusters with the representative simplified blocks in red and the real blocks in the corresponding clusters in dark grey. One hundred twenty-four blocks in Group C, F, and J pass the evaluation and filtering, and the rest are excluded for further classifications.

3.2.3. Groups by building patterns

After the survey of the building patterns of the 124 blocks, we manage to have eight building patterns derived from four of the seven basic build patterns (A through H). See Figure 8. Some of the 124 blocks are either empty (Pattern X) or under construction (Pattern U). These are an additional five building pattern types (Pattern M) which mix different building patterns as shown in Figure 6 (Pattern M1 through M5), making a total of thirteen types of building patterns. We exclude blocks that are empty or under construction for further classifications.

3.2.4. Groups by floor area ratio and site coverage ratio

The first six columns in **Table 2** shows the 29 groups resulted from this level of classification. We exclude the groups of blocks in the next two situations, regarding FAR and SCR: (1) when the mean FAR of the blocks within a group is under 3, which is the basic requirement to be qualified as high-density in Singapore; (2) when the blocks within a group contain vacant lots, which affects the calculations of the SCR. Now, we

have 23 groups of blocks. Besides, the area of the building footprints of the towers ranges from around 900 to 2’500 sqm, with the mean at around 1’800 sqm.

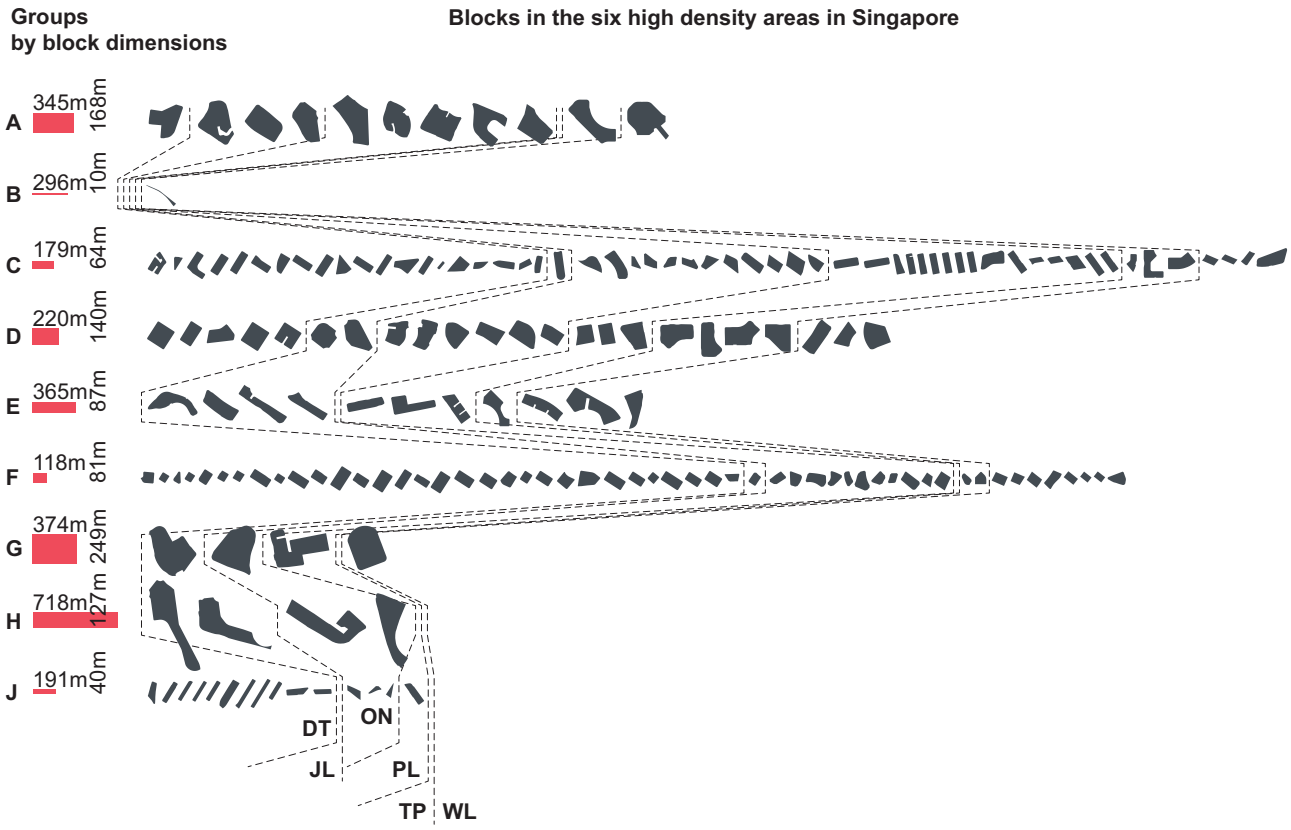

Figure 7. Nine groups of blocks by the block dimensions.

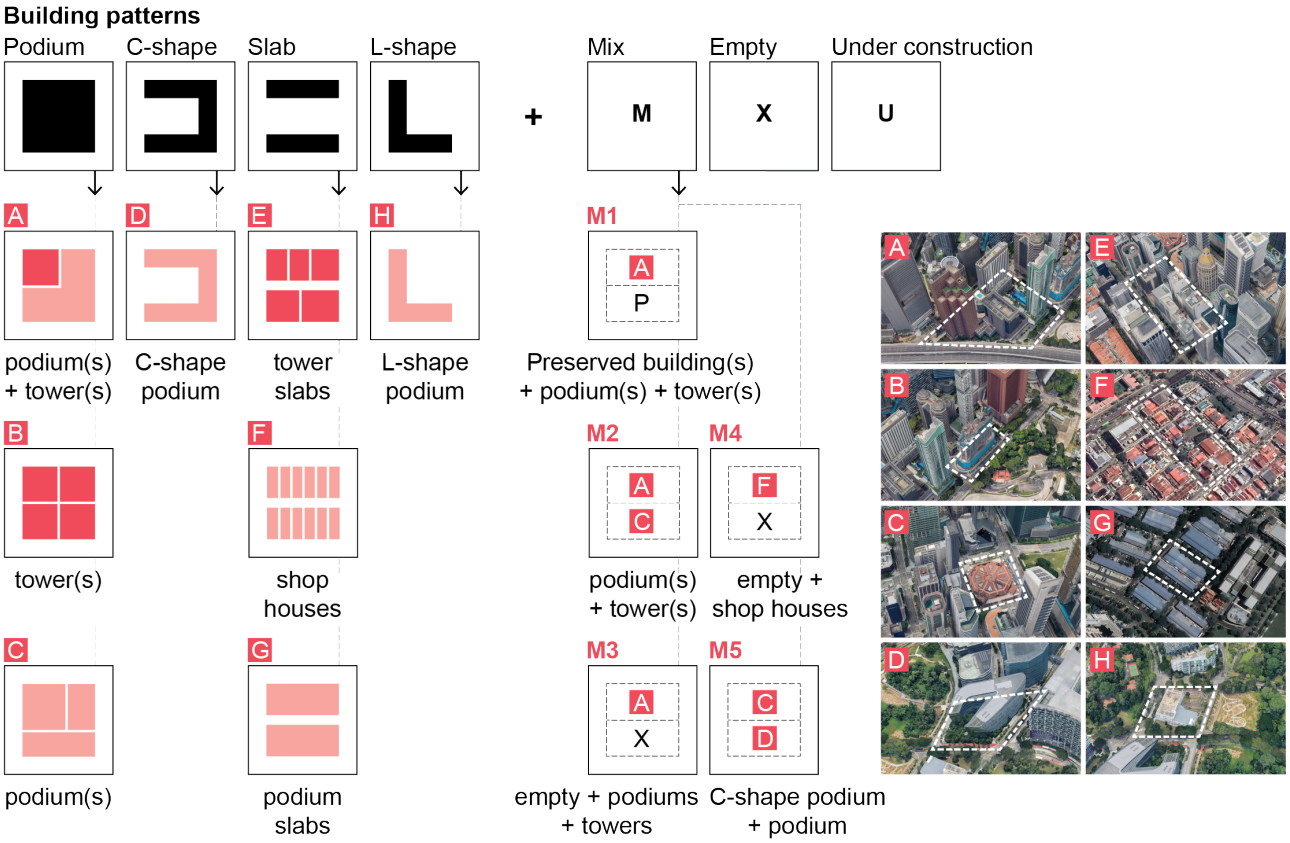

Figure 8. Thirteen types of building patterns.

3.2.5. The inventory of block typologies in high-density areas of Singapore

To define the block typologies out of the 23 groups of blocks, we conduct the last round of evaluation and selection based on the frequency of each group. The seventh column of **Table 2** counts the number of blocks that belong to that particular group. Six out of the 23 groups contain only one block, which means such a block is either unique or rare. We remove these six groups. Now, we have 18 groups of blocks, and they are numbered in the last column of **Table 2**. These 18 block typologies make up the inventory of block typologies in the six high-density areas of Singapore.

Block type	Building pattern	Number of towers, if any	FAR	SCR	Descriptions	Counts (%)	#
C	A	2-4(8)	12.8	0.9	podium(s)+tower(s)	9 (23.7%)	1
		2	8.4	0.75			2
		2-4	5.6	0.75			3
	B	1	8.4	1	tower(s)	1 (2.6%)	-
	C	-	3.6	0.4	podium(s)	9 (23.7%)	4
		-	4.5	0.75			5
	D	-	4.1	0.65	C-shape podium	2 (5.3%)	6
	E	11	11.2	0.75	tower slabs	1 (2.6%)	-
	F	-	3	0.8	shop houses	11 (28.9%)	7
	G	-	2.5	0.4	two slabs	1 (2.6%)	-
	M1	-	11.2	0.35	Preserved+podium(s) +tower(s)	1 (2.6%)	-
	M4	-	3	0.35	empty+shop houses	2 (5.3%)	-
	M5	-	2.5	0.3	C-shape podium+podium	1 (2.6%)	-
F	A	1-3	12.8	0.95	podium(s)+tower(s)	7 (29.2%)	8
		3-5	8.4	0.95			9
		1	8.4	0.6			10

	B	1-4 2-3	12 8	0.9 0.7	tower(s)	5 (20.8%)	11 12
	C	- - -	6.5 5.6 3.6	1 0.6 0.6	podium(s)	5 (20.8%)	13 14 15
	D	-	4.8	0.75	C-shape podium	1 (4.2%)	-
	G	-	2.5	0.7	two slabs	6 (25%)	-
J	A	1-5	11.4	0.9	podium(s)+tower(s)	8 (61.5%)	16
	B	6 2	11.2 4.6	0.9 0.7	tower(s)	2 (15.4%)	17 18
	M2	-	5.6	0.85	podium(s)+tower(s)	1 (7.7%)	-
	M3	-	5.6	0.45	empty+podium(s) +tower(s)	1 (7.7%)	-
	M4	-	3	0.7	empty+shop houses	1 (7.7%)	-

Table 2. The 29 groups of blocks, their features, and the 18 block typologies in the six high-density areas of Singapore.

3.3. Parametric geometric model in Grasshopper

3.3.1.Urban Block Generator for Singapore

After a series of classification in the previous chapter, we have acquired several block typologies featuring different block dimensions, building patterns, FAR, and SCR. An example of such block typology can be described as having a block dimension of around 179 m long and 64 m wide, a building pattern of podiums and two towers, with an FAR of 12.8, an SCR of 0.9. If we generate a design with such a block typology, it is easy to speculate that there are many possibilities of blocks satisfying this description. Factors causing these variances include the number of towers as well as the location of the towers and the podiums.

To solve this problem, we introduce the Urban Block Generator (UBG), a tool we develop for geometry generations on the platform of Grasshopper/Rhinoceros. The UBG can help to parametrically generate any (or random) forms of blocks that meet the description of the corresponding block typology. Figure 9 illustrates the example geometries generated by UBG. Figure 9(a) and (c) show the two possibilities of the same block typology having the same FAR, SCR, and building pattern, but different numbers and locations of the towers.

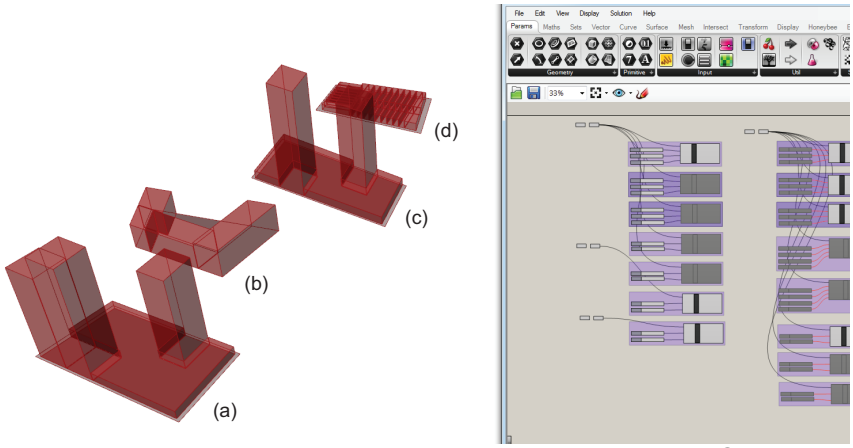

Figure 9. Example geometry generations with the Urban Block Generator.

Besides, to generate a design with block typologies, yet we need to know how the blocks are organized together. Regarding this, we adopt Shi and his colleagues' method in a recent study (Shi et al., 2019). Their method help to build a district street layout prototype where the blocks can be directly filled in. Based on a typical street grid, such a district street layout prototype takes the widths of different level of streets (arterial and minor street) into considerations. This allows more accuracy for analyses like the solar simulations, as the space in-between buildings is affected by the different street widths, which considerably influence the solar radiation (Sanaieian et al., 2014).

3.3.2.A test case in Downtown Singapore

The site of the case study is located in the north-eastern corner of the street grid of Downtown planned by the URA (Urban Redevelopment Authority, 2014b). See Figure 10(a). It contains six blocks defined by a grid street layout. For each of the six blocks, the Singapore Master Plan has restricted the limit of FAR. Figure 10(b) illustrates one of the designs generated by the UBG in Grasshopper based on the inventory of block typologies, considering the FAR restrictions. Through simulations with CEA, it is estimated that if PV panels are only applied where the annual cumulative irradiance is above 800 kWh/sqm, the overall RES achievable will be around 0.17, costing 3.48 USD/sqm for aCAPEX and 0.03 USD/sqm for OPEX on the PV system.

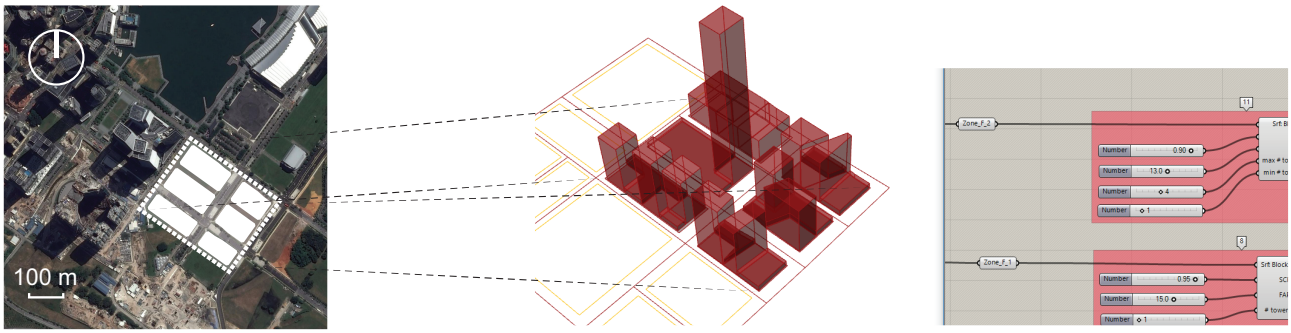

(a) (b)

Figure 10. (a) The location of the six blocks in the test case in Downtown, Singapore; (b) The design generated by UBG in Grasshopper based on the inventory of block typologies.

3.4. The results of performance assessment

3.4.1. Renewable energy resources in Singapore

There are limited renewable energy options in Singapore: low tidal range and wind speed, no hydro resources, and no economically viable geothermal energy (Energy Market Authority, 2017b). With an average annual solar irradiance of 1'580 kWh/m2/year, solar energy is the major and the most promising renewable energy source for electricity generation in Singapore (Energy Market Authority, 2017a). Besides solar energy, municipal solid waste (MSW) is another source of renewable energy resource. Incineration is the primary method of processing the non-recycled MSW in Singapore, which generates electricity from the calorific values of the MSW (Golder Associates (Singapore) Pte. Ltd, 2016).

The energy consumption fulfilled by the renewable energy sources consists of two parts: the energy consumption fulfilled by solar energy and the MSW. The energy flows of the two energy sources are illustrated in **Error! Reference source not found.**. The conversion technologies used for these two energy sources are photovoltaic panels (PV) and combined heat & power (CHP), respectively. When renewable energy resources do not suffice to fulfill all the energy consumptions, some will be prioritized over the others. Energy consumptions are prioritized in the order of space cooling, electricity, and DHW for the flows of solar energy, while DHW, space cooling, and electricity for the flows of MSW. These two orders of priority are to ensure that the energy system exhausts the renewable energy resources to fulfill the energy consumptions as much as they can. Details about the calculations of solar energy and MSW flows can be found in A and B.

For the cost calculations, this paper considers the PV alone in the cost calculations for the next reasons. One is that the investment and maintenance of a CHP are handled at the city-level far away from the HDMU areas, rather than on-site at the block-level. One is that compared to solar energy, the MSW produced in each block is very limited.

3.4.2. Results of the test case in Downtown Singapore

4. Discussion

4.1. Advantages of our method

4.2. Disadvantages of our method

4.3. Limitations and future research

This research adopts RES and the costs of the PV system as the two metrics for renewable energy potential. It is missing the third dimension – life cycle assessment. Also, we are aware that different definitions of RES may lead to fairly different results of the benchmarking. Furthermore, this research inherits the land use ratio

resulted from a previous study (Shi, Hsieh, et al., 2017). However, the land use ratio is fairly important, as it may affect the energy demand profile, the storage requirement for the electricity produced by the PV panels, and the quantity of MSW generated on-site. Lastly, in addition to the use of block typologies of the past, future research should discuss possibilities of introducing new block typologies with high renewable energy potential.
Subjective.

5. Summary

This research proposes a novel method of estimating the renewable energy potential of a greenfield project at the early stage of urban design processes with vernacular block typologies. The paper uses the City of Singapore as a demonstration. The method is implemented as a toolkit at the platform of Grasshopper/Rhinoceros, which generates a design with the inventory of block typologies in the high-density areas of Singapore and runs energy simulations with the City Energy Analyst. Additionally, this paper offers a way to interpret the results of benchmarking the renewable energy potential of the block typologies into urban design suggestions. Such suggestions help the decision-maker set achievable design boundaries, like floor area ratio, site coverage ratio or building pattern, aiming at a high or targeted renewable energy potential. Future studies shall include land use ratio and life cycle intensity as the metrics for urban design attribute and renewable energy potential.

Acknowledgments

This work was developed at the Future Cities Laboratory at the Singapore-ETH Centre, which was established collaboratively between ETH Zurich and Singapore's National Research Foundation (FI 370074016) under its Campus for Research Excellence and Technological Enterprise programme.

References

Chatzipoulka, C., Compagnon, R., & Nikolopoulou, M. (2016). Urban geometry and solar availability on façades and ground of real urban forms: Using London as a case study. *Solar Energy*, *138*, 53–66. https://doi.org/10.1016/j.solener.2016.09.005

Climate Leadership Group. (2019). *C40 CITIES*. https://www.c40.org/

Eco-Business. (n.d.). *Singapore could be 25% solar-powered by 2025*. Eco-Business. Retrieved May 9, 2019, from http://www.eco-business.com/news/singapore-could-be-25-solar-powered-by-2025/

Ellis, G., Hunter, R., Tully, M. A., Donnelly, M., Kelleher, L., & Kee, F. (2016). Connectivity and physical activity: Using footpath networks to measure the walkability of built environments. *Environment and Planning B: Planning and Design*, *43*(1), 130–151. https://doi.org/10.1177/0265813515610672

Energy Market Authority. (2017b). *Renewable Energy—Overview*. https://www.ema.gov.sg/Renewable_Energy_Overview.aspx

Energy Market Authority. (2017a). *Solar Photovoltaic Systems*. https://www.ema.gov.sg/Solar_Photovoltaic_Systems.aspx

Fonseca, J. A., Nguyen, T.-A., Schlueter, A., & Marechal, F. (2016). City Energy Analyst (CEA): Integrated framework for analysis and optimization of building energy systems in neighborhoods and city districts. *Energy and Buildings*, *113*, 202–226. https://doi.org/10.1016/j.enbuild.2015.11.055

Golder Associates (Singapore) Pte. Ltd. (2016). *Solid waste management technology roadmap*.

IEA ECBCS Annex51 - Subtask B. (2012). *Case studies on energy planning and implementation strategies for neighborhoods, quarters and municipal areas*.

Lau, K. K.-L., Lindberg, F., Johansson, E., Rasmussen, M. I., & Thorsson, S. (2017). Investigating solar energy potential in tropical urban environment: A case study of Dar es Salaam, Tanzania. *Sustainable Cities and Society*, *30*, 118–127. https://doi.org/10.1016/j.scs.2017.01.010

Li, Z., Quan, S. J., & Yang, P. P.-J. (2016). Energy performance simulation for planning a low carbon neighborhood urban district: A case study in the city of Macau. *Habitat International*, *53*, 206–214. https://doi.org/10.1016/j.habitatint.2015.11.010

Martin, L., & March, L. (1972). *Urban space and structures*. Cambridge University Press.

Merlier, L., Kuznik, F., Rusaouën, G., & Salat, S. (2018). Derivation of generic typologies for microscale urban airflow studies. *Sustainable Cities and Society*, *36*, 71–80. https://doi.org/10.1016/j.scs.2017.09.017

Mohajeri, N., Upadhyay, G., Gudmundsson, A., Assouline, D., Kämpf, J., & Scartezzini, J.-L. (2016). Effects of urban compactness on solar energy potential. *Renewable Energy*, *93*, 469–482. https://doi.org/10.1016/j.renene.2016.02.053

Montenegro, N., Duarte, J. P., & Gil, J. (2009). On the discovery of urban typologies: Data mining the many dimensions of urban form. *Proceedings of ECAADe27*, *Session 08: City Modelling 1*, 269–278. http://www.academia.edu/1483658/On_the_discovery_of_urban_typologies_data_mining_the_many_dimensions_of_urban_form

Natanian, J., Aleksandrowicz, O., & Auer, T. (2019). A parametric approach to optimizing urban form, energy balance and environmental quality: The case of Mediterranean districts. *Applied Energy*, *254*, 113637. https://doi.org/10.1016/j.apenergy.2019.113637

OpenStreetMap. (2017). *OpenStreetMap*. OpenStreetMap. https://www.openstreetmap.org/

Ratti, C., Raydan, D., & Steemers, K. (2003). Building form and environmental performance: Archetypes, analysis and an arid climate. *Energy and Buildings*, *35*(1), 49–59. https://doi.org/10.1016/S0378-7788(02)00079-8

Robert McNeel & Associates. (n.d.). *Grasshopper*. Retrieved December 4, 2019, from https://www.grasshopper3d.com/

Sanaieian, H., Tenpierik, M., Linden, K. van den, Mehdizadeh Seraj, F., & Mofidi Shemrani, S. M. (2014). Review of the impact of urban block form on thermal performance, solar access and ventilation. *Renewable and Sustainable Energy Reviews*, *38*, 551–560. https://doi.org/10.1016/j.rser.2014.06.007

Saratsis, E., Dogan, T., & Reinhart, C. F. (2017). Simulation-based daylighting analysis procedure for developing urban zoning rules. *Building Research & Information*, *45*(5), 478–491. https://doi.org/10.1080/09613218.2016.1159850

Sartori, I., Napolitano, A., & Voss, K. (2012). Net zero energy buildings: A consistent definition framework. *Energy and Buildings*, *48*, 220–232. https://doi.org/10.1016/j.enbuild.2012.01.032

SAS Institute Inc. (2016). *JMP 13* (Version 13) [Computer software].

Schirmer, P. M., & Axhausen, K. W. (2015). A multiscale classification of urban morphology. *Journal of Transport and Land Use*, *9*(1). https://doi.org/10.5198/jtlu.2015.667

Seto, K. C., Güneralp, B., & Hutyra, L. R. (2012). Global forecasts of urban expansion to 2030 and direct impacts on biodiversity and carbon pools. *Proceedings of the National Academy of Sciences of the United States of America*, *109*(40), 16083–16088.
Shi, Z., Fonseca, J. A., & Schlueter, A. (2017). A review of simulation-based urban form generation and optimization for energy-driven urban design. *Building and Environment*, *121*, 119–129. https://doi.org/10.1016/j.buildenv.2017.05.006
Shi, Z., Hsieh, S., Fonseca, J. A., & Schlueter, A. (2019). *Street layout and the cost-effectiveness of district cooling networks in high-density cities*.
Shi, Z., Hsieh, S., Sreepathi, B. K., Fonseca, J. A., & Schlueter, A. (2017). *Pilot studies on optimizing land use, building density and solar electricity generation in dense urban settings.* ISUF 2017 (the 24th International Seminar on Urban Form), Valencia, Spain.
Shields, M., & Miller, J. (2017, May 21). Swiss voters embrace shift to renewable energy. *Reuters*. https://www.reuters.com/article/us-swiss-energy-idUSKBN18H0HM
Steemers, K., Baker, N., Crowther, D., Dubiel, J., Nikolopoulou, M. H., & Ratti, C. (1997). City texture and microclimate. *Urban Design Studies*, *3*, 25–50.
The CEA team. (2018). *City Energy Analyst v2.9.0*. Zenodo. https://doi.org/10.5281/zenodo.1487867
Tsirigoti, D., & Tsikaloudaki, K. (2018). The Effect of Climate Conditions on the Relation between Energy Efficiency and Urban Form. *Energies*, *11*(3), 582. https://doi.org/10.3390/en11030582
UN-Habitat. (2012). *Energy*. http://unhabitat.org/urban-themes/energy/
United Nations. (2018). *World Urbanization Prospects, 2018 revision*. Department of Economic and Social Affairs, Population Division. https://esa.un.org/unpd/wup/Publications/Files/WUP2014-Highlights.pdf
Urban Redevelopment Authority. (2014a). *Economy*. https://www.ura.gov.sg/uol/master-plan/view-master-plan/master-plan-2014/master-plan/key-focuses/economy/economy
Urban Redevelopment Authority. (2014b). *Master Plan*. https://www.ura.gov.sg/uol/master-plan.aspx?p1=view-master-plan#
Urban Redevelopment Authority. (2014c). *URA SPACE*. https://www.ura.gov.sg/maps/?service=MP
Vartholomaios, A. (2015). The residential solar block envelope: A method for enabling the development of compact urban blocks with high passive solar potential. *Energy and Buildings*, *99*, 303–312. https://doi.org/10.1016/j.enbuild.2015.04.046
Vartholomaios, A. (2017). A parametric sensitivity analysis of the influence of urban form on domestic energy consumption for heating and cooling in a Mediterranean city. *Sustainable Cities and Society*, *28*, 135–145. https://doi.org/10.1016/j.scs.2016.09.006
Vialard, A. (2013). *A typology of block-faces* [Doctoral Thesis]. Georgia Institute of Technology.
Voss, K., Sartori, I., Napolitano, A., Geier, S., Gonçalves, H., Hall, M., Heiselberg, P., Widén, J., Candanedo, J. A., Musall, E., Karlsson, B., & Torcellini, P. (2010). Load Matching and Grid Interaction of Net Zero Energy Buildings. *EUROSUN 2010 International Conference on Solar Heating, Cooling and Buildings*. http://repositorio.lneg.pt/handle/10400.9/963
Vulkan, A., Kloog, I., Dorman, M., & Erell, E. (2018). Modeling the potential for PV installation in residential buildings in dense urban areas. *Energy and Buildings*, *169*, 97–109. https://doi.org/10.1016/j.enbuild.2018.03.052
Widén, J., Wäckelgård, E., & Lund, P. D. (2009). Options for improving the load matching capability of distributed photovoltaics: Methodology and application to high-latitude data. *Solar Energy*, *83*(11), 1953–1966. https://doi.org/10.1016/j.solener.2009.07.007
Ye, Y., Li, D., & Liu, X. (2018). How block density and typology affect urban vitality: An exploratory analysis in Shenzhen, China. *Urban Geography*, *39*(4), 631–652. https://doi.org/10.1080/02723638.2017.1381536
Zhang, J., Xu, L., Shabunko, V., Tay, S. E. R., Sun, H., Lau, S. S. Y., & Reindl, T. (2019). Impact of urban block typology on building solar potential and energy use efficiency in tropical high-density city. *Applied Energy*, *240*, 513–533. https://doi.org/10.1016/j.apenergy.2019.02.033